Development of a generalized hybrid Monte Carlo algorithm to generate the multicanonical ensemble with applications to molecular systems

Development of a generalized hybrid Monte Carlo algorithm to generate the multicanonical ensemble with applications to molecular systems

Natsuki Mukuta, and Shinichi Miura

Citation: The Journal of Chemical Physics **149**, 072322 (2018); doi: 10.1063/1.5028466
View online: https://doi.org/10.1063/1.5028466
View Table of Contents: http://aip.scitation.org/toc/jcp/149/7
Published by the American Institute of Physics

Development of a generalized hybrid Monte Carlo algorithm to generate the multicanonical ensemble with applications to molecular systems

Natsuki Mukuta[1] and Shinichi Miura[2,a)]
[1]*Graduate School of Natural Science and Technology, Kanazawa University, Kakuma, Kanazawa 920-1192, Japan*
[2]*Faculty of Mathematics and Physics, Kanazawa University, Kakuma, Kanazawa 920-1192, Japan*

(Received 10 March 2018; accepted 31 May 2018; published online 18 June 2018)

In the present paper, a generalized hybrid Monte Carlo method to generate the multicanonical ensemble has been developed, which is a generalization of the multicanonical hybrid Monte Carlo (HMC) method by Hansmann and co-workers [Chem. Phys. Lett. **259**, 321 (1996)]. The generalized hybrid Monte Carlo (GHMC) method is an equations-of-motion guided Monte Carlo combined with partial momentum refreshment. We successfully applied our multicanonical GHMC to dense Lennard-Jones fluids and a coarse grained protein model. It is found that good computational efficiency can be gained in the case of the acceptance ratio around 60% for the models examined. While a large number of molecular dynamics (MD) steps in a single GHMC cycle is needed to yield good computational efficiency at a large mixing ratio of momenta with thermal noise vectors, corresponding to the original multicanonical HMC method, a small number of MD steps are enough to achieve good efficiency at a small mixing ratio. This property is useful to develop a composite algorithm combining the present GHMC method with other Monte Carlo moves. *Published by AIP Publishing.*
https://doi.org/10.1063/1.5028466

I. INTRODUCTION

Molecular processes in the vicinity of phase transitions or in disordered systems with rugged energy landscape are widely known to be hard to sufficiently sample configurations using conventional molecular simulation techniques. In order to overcome this type of sampling problem, various enhanced sampling algorithms such as extended ensemble methods have been developed.[1–6] The multicanonical method[7,8] is a promising extended ensemble method which realizes the random walk in the potential energy space by introducing artificial statistical ensembles.[5,6] The multicanonical Monte Carlo (MC) method had originally been developed by Berg and Neuhaus;[7,8] then the molecular dynamics (MD)[9,10] and hybrid Monte Carlo (HMC)[9] algorithms to generate the multicanonical ensemble have been proposed. Compared to the conventional MD and MC methods, the multicanonical MC and MD can sample a broader range of potential energy landscape without having the system trapped in local minima; even global minimum energy configurations could be visited in a single calculation. Various methodological extensions have been carried out such as multibaric-multithermal ensembles,[11] multidimensional multicanonical ensembles,[12] and the multicanonical MD combined with the Wang-Landau sampling[13] that is called statistical temperature molecular dynamics.[14,15] Another MD method to generate an extended ensemble, the replica exchange MD method,[16] should be mentioned here. The multicanonical method and its generalization have been applied to basic Lennard-Jones systems: solid–liquid phase transition by the multicanonical method[17] and by the multibaric-multithermal method[18] and the gas–liquid interfacial tension.[19] Then, the extended ensemble methods have been applied to address various challenging problems including protein folding,[20] residual entropy of ice,[21] liquid–solid phase transition of water in finite systems,[22–24] aggregation of polymers,[25] hydration free energy change,[26] and phase diagram of a fluid in porous materials.[27]

In the present study, a generalized hybrid Monte Carlo (GHMC) algorithm to generate the multicanonical ensemble has been proposed. The hybrid Monte Carlo (HMC)[28–30] is a method that combines molecular dynamics (MD) and Monte Carlo (MC) techniques. Unlike the standard MC, whole system coordinates are simultaneously updated by equations of motion. The trial configuration generated by several molecular dynamics steps is then accepted or rejected by an appropriate Metropolis criterion as in MC. The HMC algorithm has been proved to yield the canonical distribution as long as a time-reversible and volume-preserving numerical integration algorithm is employed to solve the equations of motion.[29] The HMC method has originally been developed to solve sampling problems related with a non-ergodicity found in numerical simulations of quantum field theory.[28] Then, the method has been extended to treat condensed matters such as liquids,[29,30] including quantum many-body systems.[30–36] The canonical HMC method has been extended to generate the multicanonical ensemble by Hansmann and co-workers.[9]

a)Electronic mail: smiura@mail.kanazawa-u.ac.jp

In our preliminary study,[37] computational efficiency of the multicanonical HMC method has been examined for dense Lennard-Jones fluids and shows encouraging results. In the standard HMC method, particle momenta are randomly sampled from the Maxwell distribution at each HMC step. This condition can be relaxed so that the particle momenta are partially refreshed. This method is called the generalized hybrid Monte Carlo method.[38–41] The complete refreshment of the momenta in the standard HMC sometimes needs many molecular dynamics steps in a single HMC step to achieve good computational efficiency. The partial mixing or partial reuse of the momenta provides a possibility to achieve good computational efficiency by much a smaller number of molecular dynamics steps in a single HMC step. In the present study, the generalized hybrid Monte Carlo method for the multicanonical ensemble has been developed, trying to improve the computational efficiency of the original multicanonical HMC method. Our method is applied to dense rare gas fluids such as fluid argon and a coarse grained model of the protein molecule to examine the computational efficiency of the multicanonical GHMC method.

This paper is organized as follows. We present our method in Sec. II. Results on the dense Lennard-Jones fluid and the model protein molecule are given in Sec. III. We compare our GHMC algorithm with MD and MC algorithms in Sec. IV. Concluding remarks are given in Sec. V.

II. METHODOLOGY

A. Multicanonical ensemble

In this section, we briefly review the multicanonical ensemble method.[7,8] We consider the system consisting of N particles whose coordinates are represented by $\{\boldsymbol{r}_1, \ldots, \boldsymbol{r}_N\}$; the potential energy of the system is denoted by U. In the canonical ensemble for systems at temperature T, the distribution function $\rho_c(U, T)$ is written by

$$\rho_c(U, T) \propto \Omega(U) e^{-U/k_B T}, \tag{1}$$

where k_B is the Boltzmann constant and $\Omega(U)$ is the density of potential energy states. The distribution function has a bell-type shape whose peak is located at the ensemble average $\langle U \rangle$. The conventional Monte Carlo and molecular dynamics methods primarily sample configurations around the peak. Low energy configurations apart from the peak, for example, are hardly visited by the conventional methods. To overcome this type of sampling problems, the multicanonical method has been developed. The distribution function for the multicanonical ensemble $\rho_{mc}(U)$ is given by

$$\rho_{mc}(U) \propto \Omega(U) e^{-W(U)} = \text{constant}, \tag{2}$$

where $W(U)$ is a weight function to realize the constant distribution regarding the potential energy. The following function obviously generates the above constant distribution:

$$W(U) = \ln \Omega(U). \tag{3}$$

However, the function $\Omega(U)$ is not known *a priori*; thus, we must first numerically evaluate the weight function $W(U)$. Wang-Landau sampling,[13] for example, provides a way to evaluate the weight function. In Sec. III, another iterative numerical method will be described.

The normalization constant of the distribution function $\rho_{mc}(U)$ is given by

$$\begin{aligned} Z_{mc} &= \int dU \Omega(U) e^{-W(U)} \\ &= \int d\mathbf{r}_1 \cdots d\mathbf{r}_N e^{-W(U(\{\boldsymbol{r}_i\}))}, \end{aligned} \tag{4}$$

where $\Omega(U) = \int d\mathbf{r}_1 \cdots d\mathbf{r}_N \delta(U - U(\{\boldsymbol{r}_i\}))$. As is evident from Eq. (4), the multicanonical density in the configuration space is given by $e^{-W(U(\{\boldsymbol{r}_i\}))}$. The Metropolis Monte Carlo method, for example, can be applied to the multicanonical ensemble; the Metropolis criterion is given by $\min(1, e^{-\Delta W})$ where ΔW is the change in the function W after the trial move. In Sec. II B, we present a generalized hybrid Monte Carlo method to generate the multicanonical ensemble.

B. Generalized hybrid Monte Carlo

In the hybrid Monte Carlo method, trial configurations are generated by equations of motion. Here, we consider appropriate equations of motion to generate the multicanonical distribution. We first regard the multicanonical distribution to be a fictitious canonical distribution at a temperature T_0 using the following effective potential $U_{mc}(U)$:

$$U_{mc}(U(\{\boldsymbol{r}_i\})) = k_B T_0 W(U(\{\boldsymbol{r}_i\})). \tag{5}$$

Then, the multicanonical density can be written by $e^{-U_{mc}/k_B T_0}$; the choice of the temperature T_0 is arbitrary. The temperature T_0 is usually chosen to be the temperature corresponding to the highest energy range in flattened potential energy distribution.[10] We can readily use the canonical hybrid Monte Carlo method[28–30] and its generalization[38,39] to generate the fictitious canonical distribution described by Eq. (5). To this end, we define the following Hamiltonian H_{mc}:

$$H_{mc} = \sum_{i=1}^{N} \frac{\boldsymbol{p}_i^2}{2m_i} + U_{mc}, \tag{6}$$

where $\boldsymbol{p}_i$ is the fictitious momentum and m_i is the associated fictitious mass of an ith particle. On the basis of Hamilton's canonical equation, we obtain the following equations of motion:

$$\begin{aligned} \frac{d\boldsymbol{r}_i}{dt} &= \frac{\partial H_{mc}}{\partial \boldsymbol{p}_i} = \frac{\boldsymbol{p}_i}{m_i}, \\ \frac{d\boldsymbol{p}_i}{dt} &= -\frac{\partial H_{mc}}{\partial \boldsymbol{r}_i} = -\frac{\partial U_{mc}}{\partial U} \frac{\partial U}{\partial \boldsymbol{r}_i}. \end{aligned} \tag{7}$$

The fictitious canonical distribution in phase space

$$\pi_{mc}(\{\boldsymbol{r}_i\}, \{\boldsymbol{p}_i\}) \propto e^{-H_{mc}/k_B T_0} \tag{8}$$

is generated using the equations of motion, Eq. (7), by the generalized hybrid Monte Carlo algorithm, which consists of the following two steps: equation-of-motion guided Monte Carlo and partial momentum refreshment.

1. Equation-of-motion guided Monte Carlo

This step in turn consists of the following three parts:

(a) *Molecular dynamics*: numerically integrating Eq. (7) with a time reversible and volume preserving integrator, which is called a symplectic integrator,[42] over n_{MD} steps and time increment Δt. The map from the initial to the final state is denoted by $U_{\Delta\tau}$: $(\{\boldsymbol{r}_i\}, \{\boldsymbol{p}_i\}) \to (\{\boldsymbol{r}_i{}'\}, \{\boldsymbol{p}_i'\})$ where $\Delta\tau = n_{\mathrm{MD}} \times \Delta t$.

(b) *A momentum flip* $\mathcal{F}$: $(\{\boldsymbol{r}_i\}, \{\boldsymbol{p}_i\}) \to (\{\boldsymbol{r}_i\}, \{-\boldsymbol{p}_i\})$.

(c) *Metropolis decision*: a Metropolis acceptance/rejection criterion is applied to the trial

$$(\{\boldsymbol{r}_i'\}, \{\boldsymbol{p}_i'\}) = \begin{cases} \mathcal{F} \cdot U_{\Delta\tau}(\{\boldsymbol{r}_i\}, \{\boldsymbol{p}_i\}) & \text{with probability } \min\{1, e^{-\Delta H_{\mathrm{mc}}/k_B T_0}\} \\ (\{\boldsymbol{r}_i\}, \{\boldsymbol{p}_i\}) & \text{otherwise,} \end{cases} \tag{9}$$

where

$$\Delta H_{\mathrm{mc}} = H_{\mathrm{mc}}(\mathcal{F} \cdot U_{\Delta\tau}(\{\boldsymbol{r}_i\}, \{\boldsymbol{p}_i\})) - H_{\mathrm{mc}}(\{\boldsymbol{r}_i\}, \{\boldsymbol{p}_i\}). \tag{10}$$

It is noted that the Hamiltonian is invariant under the momentum flip

$$H_{\mathrm{mc}}(U_{\Delta\tau}(\{\boldsymbol{r}_i\}, \{\boldsymbol{p}_i\})) = H_{\mathrm{mc}}(\mathcal{F} \cdot U_{\Delta\tau}(\{\boldsymbol{r}_i\}, \{\boldsymbol{p}_i\})). \tag{11}$$

The momentum flip is needed to satisfy the detailed balance condition in the phase space since $(\mathcal{F} \cdot U_{\Delta\tau})^2 = \mathrm{id}$.

2. Partial momentum refreshment

In this step, we mix the momentum $\boldsymbol{p}$ with a Gaussian noise vector $\boldsymbol{u}$ drawn from the Maxwell distribution at the temperature T_0, which is carried out by the following equation:

$$\begin{pmatrix} \boldsymbol{p}_i' \\ \boldsymbol{u}_i' \end{pmatrix} = \begin{pmatrix} \cos\phi & \sin\phi \\ -\sin\phi & \cos\phi \end{pmatrix} \cdot \mathcal{F} \begin{pmatrix} \boldsymbol{p}_i \\ \boldsymbol{u}_i \end{pmatrix}, \quad \text{for } i = 1, \ldots, N. \tag{12}$$

Here, $\boldsymbol{u}_i$ is generated by

$$\boldsymbol{u}_i = (m_i k_B T_0)^{1/2} \boldsymbol{\xi}_i,$$

where each component of $\boldsymbol{\xi}_i$ is given by the Gaussian random number with zero mean and unit variance. The extra momentum flip $\mathcal{F}$ in Eq. (12) is included so that the trajectory is reversed on a Monte Carlo rejection instead of on an acceptance. The angle ϕ is introduced in the range of $0 < \phi \le \pi/2$. At $\phi = \pi/2$, the particle momenta $\boldsymbol{p}_i$ are fully replaced by the random momenta $\boldsymbol{u}_i$; on the other hand, at the limit of $\phi = 0$, the particle momenta are unchanged at all. At the intermediate value of ϕ, the particle momenta are partially mixed with the random momenta; the ratio of the mixing is controlled by the angle ϕ. This step does not introduce any bias to the Maxwell distribution this is easily verified as follows. For simplicity, we consider a one-dimensional case $p' = -p\cos\phi + u\sin\phi$, where both p and u obey the same Gaussian distribution with zero mean and the variance σ^2, and $3N$ dimensional extension is straightforward. The joint probability density of the independent variables p and u is written by

$$g(p, u) = \frac{1}{\sqrt{2\pi\sigma^2}} e^{-p^2/\sigma^2} \frac{1}{\sqrt{2\pi\sigma^2}} e^{-u^2/\sigma^2}. \tag{13}$$

Then, the probability density for the mixed momentum p', $f(p')$, is given by

$$\begin{aligned} f(p') &= \int dp \int du\, \delta(p' + p\cos\phi - u\sin\phi) g(p, u) \\ &= \frac{1}{\sqrt{2\pi\sigma^2}} e^{-p'^2/\sigma^2}. \end{aligned} \tag{14}$$

This clearly shows that the variable p' also obeys the same Gaussian distribution, indicating that the partial momentum refreshment step can be accepted with the probability of unity. It is noted that the case of $\phi = \pi/2$ corresponds to the standard hybrid Monte Carlo method, and the momentum flip $\mathcal{F}$ can be neglected since the momenta are fully replaced by the Gaussian random vectors.

C. Summary of the algorithm

Here, we summarize the generalized hybrid Monte Carlo (GHMC) method from the viewpoint of implementation. The algorithm is outlined as follows. We start with an initial state of the system $(\{\boldsymbol{r}_i\}, \{\boldsymbol{p}_i\})$. Each momentum $\boldsymbol{p}_i$ is mixed with a Gaussian noise vector $\boldsymbol{u}_i$ drawn from the Maxwell distribution at the temperature T_0: $\boldsymbol{p}_i \leftarrow \boldsymbol{p}_i \cos\phi + \boldsymbol{u}_i \sin\phi$ for $i = 1, \ldots, N$. Molecular dynamics based on Eq. (7) are used to move the whole system for a time increment of $n_{\mathrm{MD}} \times \Delta t$ where Δt is the time step of the MD calculation and n_{MD} is the number of MD steps in one GHMC cycle. The trial configuration is then accepted by the probability $\min\left(1, e^{-\Delta H_{\mathrm{mc}}/k_B T_0}\right)$ where ΔH_{mc} is the change in the total Hamiltonian H_{mc} after the move of n_{MD} steps. If the trial configuration is rejected, the momentum must be negated,

$$(\{\boldsymbol{r}_i'\}, \{\boldsymbol{p}_i'\}) = (\{\boldsymbol{r}_i\}, \{-\boldsymbol{p}_i\}). \tag{15}$$

Here, the above momentum reversal is the result of the operation of $\mathcal{F}$ in Eq. (12).

III. RESULTS

A. Lennard-Jones fluid

We first present results on the applications of our method to dense rare gas fluids. The fluid system is composed of $N = 108$ particles interacting with the Lennard-Jones potential. The following potential parameters appropriate for argon are adopted: $\sigma = 3.41$ Å and $\epsilon/k_B = 120$ K. Density of the system is set to be $\rho = 0.022\,37$ Å^{-3}, corresponding to high

density states near the triple point of the liquid argon; temperature T_0 = 180 K for the fictitious canonical ensemble with the multicanonical effective potential $U_{\rm mc}$, Eq. (5). To calculate the force appeared in Eq. (7), the coefficient $\partial U_{\rm mc}/\partial U$ is numerically evaluated using the Lagrangian cubic interpolation technique. Using the multicanonical effective potential described below, we performed 1.0×10^5 GHMC steps for various tunable parameters to discuss the computational efficiency; we used a velocity Verlet algorithm[43,44] to numerically integrate the equations of motion.

To perform the multicanonical GHMC calculations, we must first numerically evaluate the multicanonical weight function $W(U)$. An initial guess on the weight function $W(U)$ can be evaluated using the canonical distribution at a temperature T_0,

$$W(U) = \ln \Omega(U) = \frac{U}{k_B T_0} + \ln \rho_{\rm c}(U, T_0), \tag{16}$$

where energy independent terms are omitted. To obtain the function $W(U)$, we performed 10 000 GHMC steps with parameters $\phi = \pi/2$, $n_{\rm MD} = 10$, and $\Delta t = 35$ fs. Since the numerical canonical simulation for the temperature T_0 does not cover a sufficiently broad U range, we must refine the function $W(U)$ iteratively using the following relation:

$$W^{(n+1)}(U) = W^{(n)}(U) + \ln \rho_{\rm mc}^{(n)}(U), \tag{17}$$

where the nth multicanonical distribution $\rho_{\rm mc}^{(n)}(U)$ is obtained by the weight function $W^{(n)}(U)$. About 1000 iterations are needed to obtain a sufficiently flat energy distribution: a criterion to terminate the iteration is that the difference between the height of adjacent bins in the energy histogram is less than 0.3 in the logarithmic scale. Detailed description on the method of the refinement can be found in Ref. 6. The distribution using the refined $W(U)$ is presented in Fig. 1. In the energy range $[-637.2\epsilon, -540\epsilon]$, a flat distribution is found to be obtained. Outside the range, the system is designed to obey the canonical distribution. The energy range flattened corresponds to thermodynamic states covering from near the triple point to the supercritical condition. The averaged potential energy evaluated by the reweighting technique can be found for the fluid system in Ref. 37. This weight function $W(U)$ is used to perform GHMC calculations for examining the computational efficiency.

We next discuss the computational efficiency of the multicanonical GHMC method. We examine the sampling efficiency using a quantity called a statistical inefficiency,[45,46] which is also called an integrated autocorrelation time.[47,48] This quantity expresses the number of correlated steps needed to obtain independent sampling for a physical quantity. The statistical inefficiency is different for different physical quantities. Therefore, in the present study, we deal with the efficiency for estimating a specific quantity, which is chosen to be the potential energy. We calculate the statistical inefficiency in units of the number of GHMC steps. We define the correlation time τ as the CPU time taken to compute the correlated GHMC steps. We first show the results on the GHMC calculations with $\phi = \pi/2$ corresponding to the standard HMC algorithm. In Fig. 2, we present the time step Δt dependence of the correlation time for $n_{\rm MD} = 10$. The associated acceptance ratio is also presented. If the equations of motion are accurately integrated, corresponding to the high acceptance ratio, the movement in the phase space is small; this results in the long correlation. On the other hand, if we adopt large Δt corresponding to the low acceptance ratio, the system moves widely in the phase space; however, many of the trial configurations are rejected due to the large Hamiltonian error resulting in the long correlation again. Thus, the correlation time τ has a minimum value between the high and low acceptance ratios. As seen in Fig. 2, the minimum correlation is given by $\Delta t = 35$ fs; the corresponding acceptance ratio is found to be 55%. In Fig. 3, the correlation time and the associated acceptance ratio are presented for various $n_{\rm MD}$ with $\Delta t = 35$ fs. We find that the case of $n_{\rm MD} = 10$ yields the minimum τ. The trend is similar with that found for canonical HMC calculations of dense LJ fluids;[29] however, the acceptance ratio around 70% is demonstrated to be efficient for the canonical HMC calculations. On the other hand, the smaller acceptance ratio gives a better efficiency for the multicanonical ensemble. This could be partly due to the fact that Δt giving the good efficiency depends on the energy

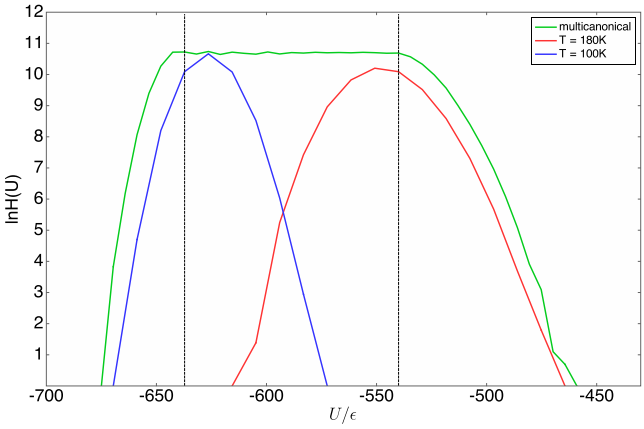

FIG. 1. Unnormalized histogram of potential energy U, $H(U)$, for the multicanonical ensemble is plotted in the logarithmic scale, together with the canonical results at temperatures T = 180 K and 100 K for comparison. While the distribution is tuned to be flat inside dashed vertical lines, the distribution is designed to obey the canonical distribution outside the range.

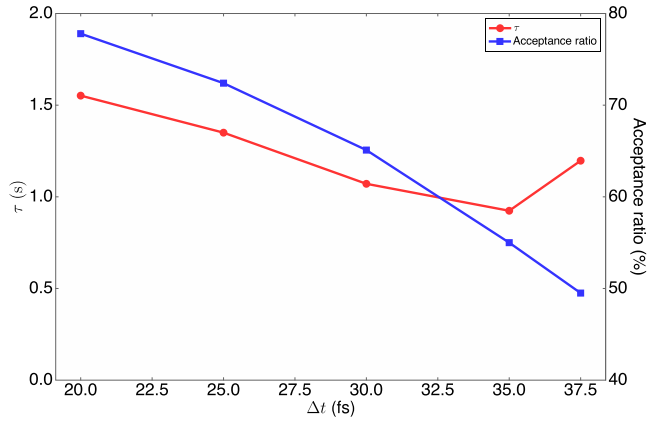

FIG. 2. The correlation time τ for the potential energy is presented as a function of Δt for the following GHMC parameters: $\phi = \pi/2$ and $n_{\rm MD} = 10$. The associated acceptance ratio is also presented as a function of Δt.

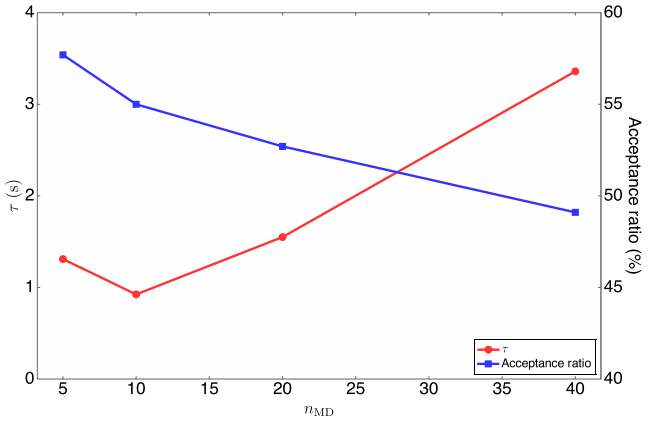

FIG. 3. The correlation time τ for the potential energy is presented as a function of n_{MD} for the following GHMC parameters: $\phi = \pi/2$ and $\Delta t = 35$ fs. The associated acceptance ratio is also presented as a function of n_{MD}.

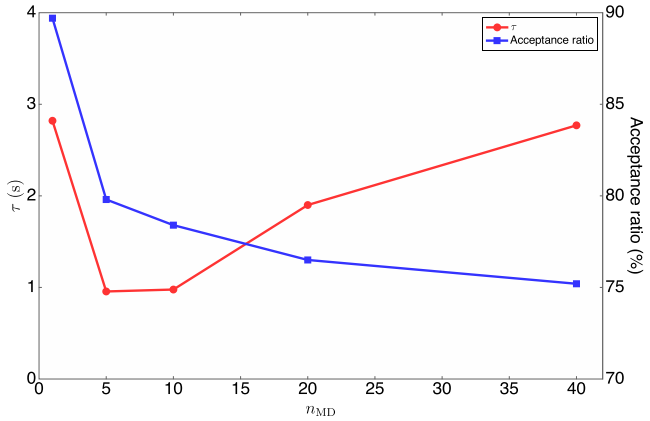

FIG. 5. The correlation time τ for the potential energy is presented as a function of n_{MD} for the following GHMC parameters: $\phi = \pi/4$ and $\Delta t = 35$ fs. The associated acceptance ratio is also presented as a function of n_{MD}.

range, which covers from low to high temperature systems, as seen in Fig. 1.

We next show the mixing angle ϕ dependence of the computational efficiency. The parameter Δt and n_{MD} are first fixed to be 35 fs and 10, respectively. We show the ϕ dependence of the correlation time τ in Fig. 4. The acceptance ratio is found to be independent of ϕ because the initial momenta obeying the Maxwell distribution do not affect the accuracy of the integration of the equations of motion. The correlation time τ becomes shorter as the mixing angle ϕ increases. The minimum τ is given in the case of $\phi = \pi/2$ where the momenta are fully refreshed at each GHMC step, which corresponds to the standard HMC algorithm. In order to see the n_{MD} dependence for other ϕ, we show the correlation time τ for various n_{MD} with $\phi = \pi/4$ and $\Delta t = 35$ fs in Fig. 5. We find that the case of $n_{MD} = 5$ yields the minimum τ, which is comparable with τ in the case of $\phi = \pi/2$ and $n_{MD} = 10$. For the dense LJ fluid, efficiency can be gained using a smaller number of n_{MD} in the case of partial momentum refreshment.

B. Coarse grained protein model

In this section, we consider a coarse grained model of a protein molecule that is a Honeycutt-Thirumalai β-barrel *BLN* model,[49] denoted by the *βBLN* model. This model is chosen to be a testing system for our multicanonical GHMC method since the model has been extensively studied and provides a good example of a rugged energy landscape.[50–54] The model molecule is composed of three types of beads: hydrophobic (B), hydrophilic (L), and neutral (N). In the present study, a *βBLN* 46-mer is chosen as a model system whose primary sequence is $B_9N_3(LB)_4N_3B_9N_3(LB)_5L$. The potential energy includes the following terms: bond-length, bond-angle, torsion-dihedral, and nonbonded potential terms. The explicit expression of the potential functions and their parameters can be found in Ref. 53. The global minimum energy structure is known to be given by a β-barrel structure with an energy of −49.2673. Here and hereafter, we describe properties of the model using the reduced units based on the potential parameters. We first evaluated the weight function $W(U)$ iteratively, as described in Sec. III A. At each iteration, we performed 1 000 000 GHMC steps with $n_{MD} = 10$, $\Delta t = 0.025$, and $\phi = \pi/8$. A criterion to terminate the iteration is that the difference between the height of adjacent bins in the energy histogram is less than 0.2 in the logarithmic scale. 66 iterations are needed to satisfy

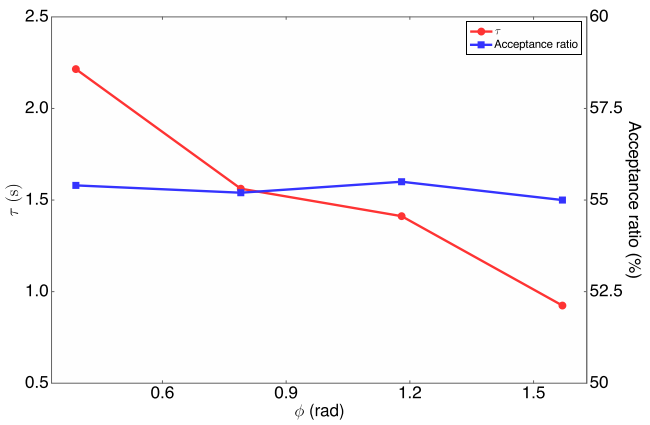

FIG. 4. The correlation time τ for the potential energy is presented as a function of the mixing angle ϕ for the following GHMC parameters: $\Delta t = 35$ fs and $n_{MD} = 10$. The associated acceptance ratio is also presented as a function of ϕ.

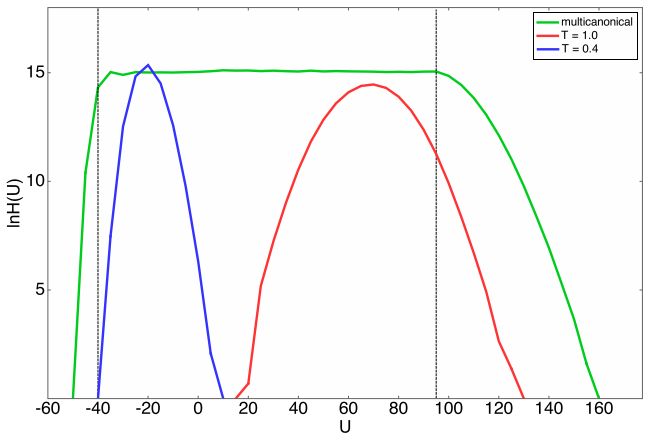

FIG. 6. Unnormalized histogram of the potential energy U, $H(U)$, for the multicanonical ensemble is plotted in the logarithmic scale, together with the canonical results at temperatures $T = 0.4$ and 1.0 for comparison. While the distribution is tuned to be flat inside dashed vertical lines, the distribution is designed to obey the canonical distribution outside the range. Physical quantities are represented in the reduced units of the model.

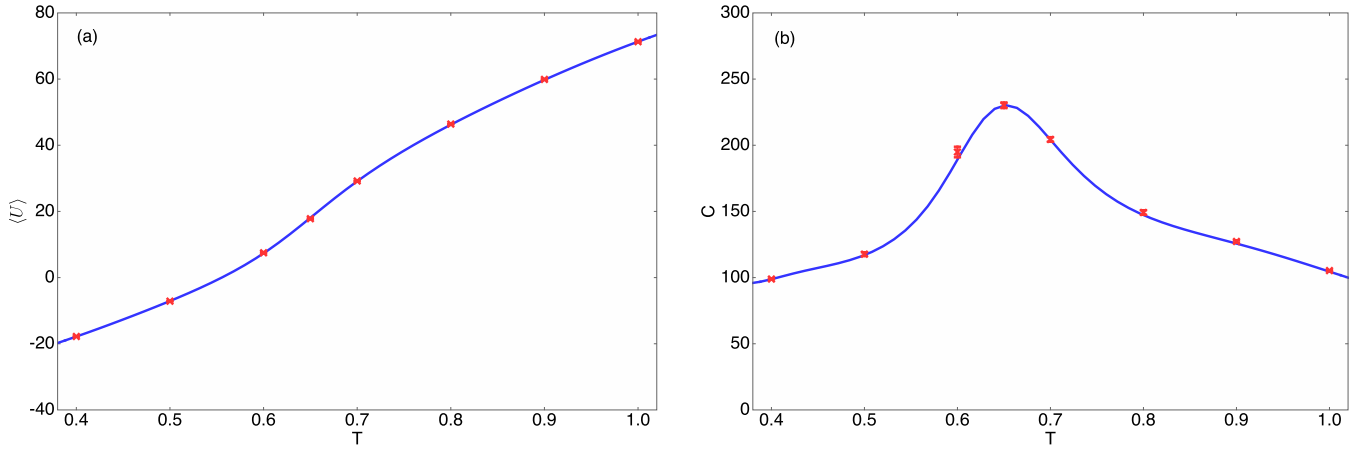

FIG. 7. Panel (a): The average potential energy $\langle U \rangle$ as a function of the temperature T is presented. The blue curve is obtained by the multicanonical GHMC calculation with the reweighting technique. Red crosses are the results of the separate canonical GHMC calculations. Error bars for the canonical GHMC results are smaller than the size of the cross symbols. Panel (b): The specific heat C as a function of the temperature T is presented. The blue curve is obtained by the multicanonical calculation with the reweighting technique. Red crosses are the results of the separate canonical GHMC calculations. Error bars for the canonical GHMC results are smaller than the size of the cross symbols. Physical quantities are represented in the reduced units of the model in both the panels.

the criterion. In Fig. 6, a flat distribution is demonstrated to be obtained in the energy range [−40, 95]. For each multicanonical GHMC run, 1.0×10^7 GHMC steps have been carried out; we used a velocity Verlet algorithm[43,44] to numerically integrate the equations of motion.

We first present the canonical average of physical quantities for this model protein molecule. The canonical average is obtained from the multicanonical GHMC results using the reweighting technique. The canonical distribution $\rho_c(U, T)$ is represented by the multicanonical distribution $\rho_{mc}(U)$,

$$\rho_c(U,T) \propto \rho_{mc}(U) e^{W(U)-U/k_BT}. \tag{18}$$

Then, the canonical average of a physical quantity $A(U)$ is estimated by

$$\langle A(U) \rangle = \frac{\int dU A(U) \rho_{mc}(U) e^{W(U)-U/k_BT}}{\int dU \rho_{mc}(U) e^{W(U)-U/k_BT}}. \tag{19}$$

In Fig. 7, we present the averaged potential energy as a function of the temperature T using the above reweighting technique with $A(U) = U$; results of independent canonical GHMC calculations are also presented for comparison. For all the temperature ranges presented, the reweighted results are in excellent agreement with the canonical GHMC results. In Fig. 7, the specific heat associated with the potential energy fluctuation is also presented. The specific heat C is calculated by

$$C = \frac{1}{k_B T^2} \left\langle (U - \langle U \rangle)^2 \right\rangle = \frac{1}{k_B T^2} \left(\langle U^2 \rangle - \langle U \rangle^2 \right). \tag{20}$$

The average $\langle U^2 \rangle$ is also evaluated by the reweighting technique. The specific heat as a function of the temperature is found to have a peak around $T = 0.65$, which is generated by the steep decrease of the averaged potential energy with lowering of the temperature. This peak signals the collapse transition from a random coil to collapse states.[52,54] The reweighted results are found to be again in perfect agreement with the canonical GHMC results. It is worthwhile to note that the temperature range targeted by the reweighting method must be well inside the temperature range covered by the flattened potential energy distribution.

We discuss the computational efficiency of the multicanonical GHMC method. We first show the results in the case of the mixing angle $\phi = \pi/2$ corresponding to the standard HMC algorithm. In Fig. 8, we show the time step Δt dependence of the correlation time τ together with the associated acceptance ratio. The parameter n_{MD} is first fixed to be 10. For this coarse grained protein model, the minimum τ is found to be given by $\Delta t = 0.025$. The corresponding acceptance ratio is 63%. In Fig. 9, the correlation time and the associated acceptance ratio are presented for various n_{MD} with $\Delta t = 0.025$. We find a plateau region in the n_{MD} dependence for $n_{MD} = 40$–150. In any case, the optimum n_{MD} is larger than that in the case of the dense LJ fluids. This type of a trend has been observed for the canonical HMC calculations applied to isolated molecules[36] and medium and low density fluids for canonical calculations.[35,55] Although intermediate configurations are usable to evaluate statistical

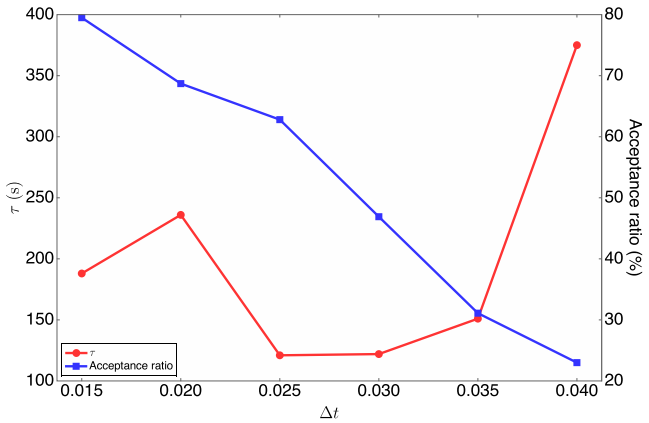

FIG. 8. The correlation time τ for the potential energy is presented as a function of Δt for the following GHMC parameters: $\phi = \pi/2$ and $n_{MD} = 10$. Physical quantities are represented in the reduced units of the model. The associated acceptance ratio is also presented as a function of Δt.

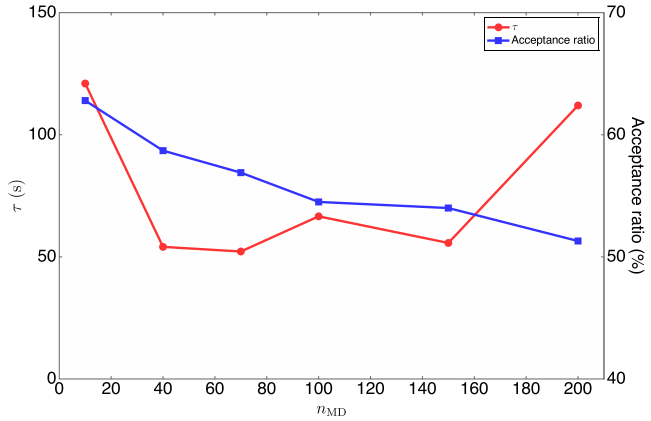

FIG. 9. The correlation time τ for the potential energy is presented as a function of n_{MD} for the following GHMC parameters: $\phi = \pi/2$ and $\Delta t = 0.025$. Physical quantities are represented in the reduced units of the model. The associated acceptance ratio is also presented as a function of n_{MD}.

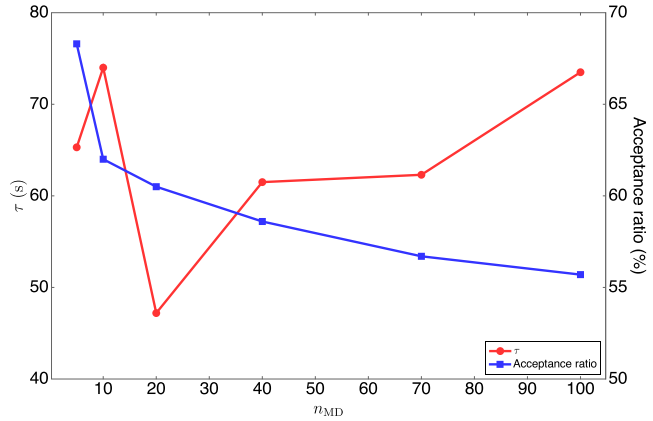

FIG. 11. The correlation time τ for the potential energy is presented as a function of n_{MD} for the following GHMC parameters: $\phi = \pi/8$ and $\Delta t = 0.025$. Physical quantities are represented in the reduced units of the model. The associated acceptance ratio is also presented as a function of n_{MD}.

averages of physical quantities,[35,55] it is better to use smaller n_{MD} to efficiently be combined with other Monte Carlo trial moves from the viewpoint of balancing computational costs.

We next show the computational efficiency for various mixing angles ϕ. The parameter Δt and n_{MD} are first fixed to be 0.025 and 10, respectively. In Fig. 10, we indicate the ϕ dependence of the correlation time τ and the associated acceptance ratio. The minimum correlation is found to be given by $\phi = \pi/8$. The corresponding acceptance ratio is 62%. It is efficient to mix a random momentum from the Maxwell distribution by approximately 40% for this protein model, and it is about half the correlation time as compared with the case of $\phi = \pi/2$. In Fig. 11, the correlation time is presented for various n_{MD}. The parameter ϕ and Δt are fixed to be $\pi/8$ and 0.025, respectively. We find that the case of $n_{MD} = 20$ yields minimum correlation time. As found in dense LJ fluids, we can obtain good efficiency using smaller n_{MD} by the partial momentum refreshment. As mentioned in Sec. III A, the statistical inefficiency or the integrated autocorrelation time depends on a physical quantity selected to measure. We have

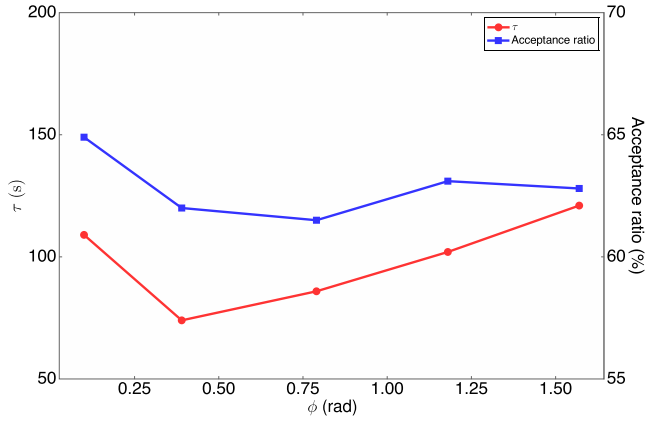

FIG. 10. The correlation time τ for the potential energy is presented as a function of the mixing angle ϕ for the following GHMC parameters: $\Delta t = 0.025$ and $n_{MD} = 10$. Physical quantities are represented in the reduced units of the model. The associated acceptance ratio is also presented as a function of ϕ.

also estimated the statistical inefficiency of another physical quantity, the square of the potential energy U^2 which appears in the expression of the specific heat Eq. (20). We found that the statistical inefficiency of U^2 shows almost the same Δt, n_{MD}, and ϕ dependences with that of U presented above; the optimal mixing angle on U^2 is confirmed to be the same as that on U.

IV. DISCUSSION

In this section, we compare our generalized hybrid Monte Carlo (GHMC) method with other related molecular simulation methods for the multicanonical ensemble. We first discuss the molecular dynamics (MD) method. In the MD method, equations of motion are modified by attaching a thermostat to generate the fictitious canonical distribution in the phase space.[10] In the GHMC method, given the partially refreshed momenta, system coordinates evolve according to the equations of motion; trial configurations are accepted so as to be compatible with Eq. (8). According to our experience on the canonical HMC, it is possible to get better computational efficiency than MD using suitably chosen HMC parameters n_{MD} and Δt. Usually, larger Δt than that of MD can be used in HMC calculations; biases introduced by the resulting Hamiltonian error are removed by the appropriate Metropolis criterion. Optimized HMC parameters and comparison on the computational efficiency can be found, for example, for standard Lennard-Jones fluids[29] and quantum many-body systems described by the path integral method.[31,36] As far as the multicanonical MD is concerned, it is known to be needed to use a rather small time step Δt for stable numerical calculations.[9,56] As mentioned above, the equations of motion are not necessary to be accurately solved in the GHMC method. In the present study, it is found that we can safely use a large Δt for efficient GHMC calculations. Additionally, in order to solve the thermostatted equations of motion, we need to provide an inertial quantity or "mass" of the heat bath. The optimal choice of the mass is given on the basis of the characteristic frequency of the system considered.[57–59] Since the force in the multicanonical MD is modified by the factor associated with the multicanonical weight, it is difficult to properly

evaluate the inertial quantity prior to MD calculations. To our best knowledge, the method of the choice on the inertial quantity is not well established for the multicanonical MD.

We move on to the comparison with the standard Monte Carlo method using local moves. To our experience, in general, the computational efficiency by the standard Monte Carlo is comparable with and even better than that by the hybrid Monte Carlo. Here, we summarize the advantages of the hybrid Monte Carlo method, which are not present in the local move MC. In HMC, unlike the standard MC method, all the coordinates are simultaneously updated; this feature enables us to use efficient parallel computation algorithms developed for MD,[60] which are useful to perform large scale HMC simulations. This global update of the coordinates is also advantageous to perform calculations of systems described by many-body interactions including, for example, induced dipole moments of molecules and even by combining with electronic structure calculations.

V. CONCLUDING REMARKS

In the present paper, we have developed the generalized hybrid Monte Carlo (GHMC) algorithm to generate the multicanonical ensemble. Our method is a generalization of the hybrid Monte Carlo method developed by Hansmann and co-workers.[9] Dense Lennard-Jones fluids and a coarse grained protein model are chosen to be model systems to examine computational efficiency. There are three tunable parameters for the GHMC calculations: determining the ratio of the momentum mixing with a random noise vector ϕ, number of molecular dynamics steps per unit GHMC cycle n_{MD}, and the time increment to numerically integrate equations of motion Δt. The mixing angle $\phi = \pi/2$ corresponds to the multicanonical HMC algorithm given by Hansmann and co-workers,[9] where the momenta are fully refreshed at each GHMC step. In the case of $\phi = \pi/2$, computational efficiency of the multicanonical GHMC shows the similar trend found in the canonical counterpart; however, the acceptance ratio yielding good efficiency is somewhat smaller than that of the canonical HMC. This could arise from a factor that appeared in the force evaluation, which is associated with the multicanonical weight. By changing the mixing angle ϕ, we can gain better efficiency for smaller n_{MD} compared with that at $\phi = \pi/2$; this trend is more remarkable for the model protein molecule. This property is, for example, useful to combine the GHMC method with the replica exchange technique[61,62] from the viewpoint of balancing computational costs.

ACKNOWLEDGMENTS

We would like to thank Tsugumichi Tagawa for fruitful discussions on the multicanonical calculations.

[1] D. Frenkel and B. Smit, *Understanding Molecular Simulation: From Algorithms to Applications*, 2nd ed. (Academic Press, San Diego, 2002).
[2] K. Binder and D. Heermann, *Monte Carlo Simulation in Statistical Physics*, 5th ed. (Springer, New York, 2010).
[3] M. E. Tuckerman, *Statistical Mechanics: Theory and Molecular Simulation* (Oxford University Press, New York, 2010).
[4] D. P. Landau and K. Binder, *A Guide to Monte Carlo Simulations in Statistical Physics*, 4th ed. (Cambridge University Press, Cambridge, 2015).
[5] U. H. E. Hansmann and Y. Okamoto, Curr. Opin. Struct. Biol. **9**, 177 (1999).
[6] B. A. Berg, Fields Inst. Commun. **26**, 1 (2000).
[7] B. A. Berg and T. Neuhaus, Phys. Lett. B **267**, 249 (1991).
[8] B. A. Berg and T. Neuhaus, Phys. Rev. Lett. **68**, 9 (1992).
[9] U. H. E. Hansmann, Y. Okamoto, and F. Eisenmenger, Chem. Phys. Lett. **259**, 321 (1996).
[10] N. Nakajima, H. Nakamura, and A. Kidera, J. Phys. Chem. B **101**, 817 (1997).
[11] H. Okumura and Y. Okamoto, Chem. Phys. Lett. **383**, 391 (2004).
[12] A. Mitsutake and Y. Okamoto, Phys. Rev. E **79**, 047701 (2009).
[13] F. Wang and D. P. Landau, Phys. Rev. Lett. **86**, 2050 (2001).
[14] J. Kim, J. E. Straub, and T. Keyes, Phys. Rev. Lett. **97**, 050601 (2006).
[15] J. Kim, J. E. Straub, and T. Keyes, J. Chem. Phys. **126**, 135101 (2007).
[16] Y. Sugita and Y. Okamoto, Chem. Phys. Lett. **314**, 141 (1999).
[17] C. Muguruma, Y. Okamoto, and M. Mikami, J. Chem. Phys. **120**, 7557 (2004).
[18] T. Kaneko, A. Mitsutake, and K. Yasuoka, J. Phys. Soc. Jpn. **81**(Suppl. A), SA014 (2012).
[19] J. J. Potoff and A. Z. Panagiotopoulos, J. Chem. Phys. **112**, 6411 (2000).
[20] A. Mitsutake, Y. Sugita, and Y. Okamoto, Biopolymers **60**, 96 (2001).
[21] B. A. Berg, C. Muguruma, and Y. Okamoto, Phys. Rev. B **75**, 092202 (2007).
[22] T. Kaneko, J. Bai, K. Yasuoka, A. Mitsutake, and X. C. Zeng, J. Chem. Phys. **140**, 184507 (2014).
[23] T. Kaneko, J. Bai, K. Yasuoka, A. Mitsutake, and X. C. Zeng, J. Chem. Theory Comput. **9**, 3299 (2013).
[24] T. Kaneko, T. Akimoto, K. Yasuoka, A. Mitsutake, and X. C. Zeng, J. Chem. Theory Comput. **7**, 3083 (2011).
[25] J. Zierenberg, M. Mueller, P. Schierz, M. Marenz, and W. Janke, J. Chem. Phys. **141**, 114908 (2014).
[26] H. Doi and M. Aida, Chem. Phys. Lett. **595**, 55 (2014).
[27] V. De Grandis, P. Gallo, and M. Rovere, Europhys. Lett. **75**, 901 (2006).
[28] S. Duane, A. D. Kennedy, B. J. Pendleton, and D. Roweth, Phys. Lett. B **195**, 216 (1987).
[29] B. Mehlig, D. W. Heermann, and B. M. Forrest, Phys. Rev. B **45**, 679 (1992).
[30] M. Tuckerman, B. J. Berne, G. J. Martyna, and M. L. Klein, J. Chem. Phys. **99**, 2796 (1993).
[31] S. Miura and J. Tanaka, J. Chem. Phys. **120**, 2160 (2004).
[32] S. Miura, J. Phys.: Condens. Matter **17**, S3259 (2005).
[33] S. Miura, J. Chem. Phys. **126**, 114308 (2007).
[34] S. Miura, J. Chem. Phys. **126**, 114309 (2007).
[35] S. Miura, in *Advances in Quantum Monte Carlo*, The ACS Symposium Series, edited by S. Tanaka, S. Rothstein, and W. Lester (American Chemical Society, Washington, DC, 2012), Vol. 1094, Chap. 14, pp. 177–186.
[36] Y. Kamibayashi and S. Miura, J. Chem. Phys. **145**, 074114 (2016).
[37] T. Tagawa, T. Kaneko, and S. Miura, Mol. Simul. **43**(13), 1291 (2017).
[38] A. M. Horowitz, Phys. Lett. B **268**, 247 (1991).
[39] A. D. Kennedy and B. Pendleton, Nucl. Phys. B **607**, 456 (2001).
[40] E. Akhmatskaya, N. Bou-Rabee, and S. Reich, J. Comput. Phys. **228**, 2256 (2009).
[41] E. Akhmatskaya, N. Bou-Rabee, and S. Reich, J. Comput. Phys. **228**, 7492 (2009).
[42] E. Hairer, C. Lubich, and G. Wanner, *Geometric Numerical Integration*, 2nd ed. (Springer, Heidelberg, 2006).
[43] W. C. Swope, H. C. Andersen, P. H. Berens, and K. R. Wilson, J. Chem. Phys. **76**, 637 (1982).
[44] M. Tuckerman, B. J. Berne, and G. J. Martyna, J. Chem. Phys. **97**, 1990 (1992).
[45] R. Friedberg and J. E. Cameron, J. Chem. Phys. **52**, 6049 (1970).
[46] M. P. Allen and D. J. Tildesley, *Computer Simulation of Liquids* (Clarendon, Oxford, 1987).
[47] A. Sokal, in *Functional Integration: Basics and Applications*, edited by C. DeWitt-Morette, P. Cartier, and A. Folacci (Plenum Press, New York, 1997).
[48] B. Berg, *Markov Chain Monte Carlo Simulations and Their Statistical Analysis* (World Scientific, Singapore, 2004).
[49] J. F. Honeycutt and D. Thirumalai, Proc. Natl. Acad. Sci. U. S. A. **87**, 3526 (1990).

[50]C. J. Camacho and D. Thirumalai, Proc. Natl. Acad. Sci. U. S. A. **90**, 6369 (1993).
[51]D. Klimov and D. Thirumalai, Phys. Rev. Lett. **76**, 4070 (1996).
[52]Z. Guo and C. L. Brooks III, Biopolymers **42**, 745 (1997).
[53]Y.-H. Lee and B. J. Berne, J. Phys. Chem. A **104**, 86 (2000).
[54]F. Calvo and J. P. K. Doye, Phys. Rev. E **63**, 010902 (2000).
[55]N. Matubayasi and M. Nakahara, J. Chem. Phys. **110**, 3291 (1999).
[56]H. Shimizu, Phys. Rev. E **70**, 056704 (2004).
[57]S. Nosé, J. Chem. Phys. **81**, 511 (1984).
[58]G. J. Martyna, M. L. Klein, and M. J. Tuckerman, J. Chem. Phys. **97**, 2635 (1992).
[59]G. J. Martyna, M. E. Tuckerman, D. J. Tobias, and M. L. Klein, Mol. Phys. **87**, 1117 (1996).
[60]S. Plimpton, J. Comput. Phys. **117**, 1 (1995).
[61]K. Hukushima and K. Nemoto, J. Phys. Soc. Jpn. **65**, 1604 (1996).
[62]E. Marinari, G. Parisi, and J. J. Ruiz-Lorenzo, in *Spin Glasses and Random Fields*, edited by A. P. Young (World Scientific, New Jersey, 1998).